

Kaluza-Klein Dark Matter

Hsin-Chia Cheng,¹ Jonathan L. Feng,² and Konstantin T. Matchev^{3,4}

¹*Enrico Fermi Institute, The University of Chicago, Chicago, Illinois 60637*

²*Department of Physics and Astronomy, University of California, Irvine, California 92697*

³*Department of Physics, University of Florida, Gainesville, Florida 32611*

⁴*Theory Division, CERN, CH-1211 Geneva, Switzerland*

(Received 12 July 2002; revised manuscript received 10 September 2002; published 30 October 2002)

We propose that cold dark matter is made of Kaluza-Klein particles and explore avenues for its detection. The lightest Kaluza-Klein state is an excellent dark matter candidate if standard model particles propagate in extra dimensions and Kaluza-Klein parity is conserved. We consider Kaluza-Klein gauge bosons. In sharp contrast to the case of supersymmetric dark matter, these annihilate to hard positrons, neutrinos, and photons with unsuppressed rates. Direct detection signals are also promising. These conclusions are generic to bosonic dark matter candidates.

DOI: 10.1103/PhysRevLett.89.211301

PACS numbers: 95.35.+d, 11.10.Kk, 12.60.-i

The identity of dark matter is currently among the most profound mysteries in particle physics, astrophysics, and cosmology. Recent data from supernovae luminosities, cosmic microwave anisotropies, and galactic rotation curves all point consistently to the existence of dark matter with mass density $\Omega \approx 0.3$ relative to the critical density. At the same time, all known particles are excluded as dark matter candidates, making the dark matter problem the most pressing phenomenological motivation for particles and interactions beyond the standard model.

Among the myriad options, the possibility of particle dark matter with weak interactions and weak-scale mass is particularly tantalizing. Puzzles concerning electroweak symmetry breaking suggest that such particles exist, and, if stable, their thermal relic density is generically in the desired range. Among these candidates, neutralinos in supersymmetric theories are by far the most widely studied. Neutralinos have spin 1/2 and are their own antiparticles; that is, they are Majorana fermions. They may be detected directly through scattering in detectors, or indirectly through the decay products that result when neutralinos annihilate in pairs. For indirect detection, however, the Majorana nature of neutralinos implies that annihilation is chirality suppressed, leading to soft secondary positrons, photons, and neutrinos, and considerably diminishing prospects for discovery.

Here we study a specific example of a generic alternative: bosonic cold dark matter. If particles propagate in extra spacetime dimensions, they will have an infinite tower of partner states with identical quantum numbers, as noted long ago by Kaluza and Klein [1]. We consider the case of universal extra dimensions (UED) [2], in which all standard model particles propagate. Such models provide, in the form of stable Kaluza-Klein (KK) partners, the only specific dark matter candidate to emerge from theories with extra dimensions [3–5]. KK dark matter generically has the desired relic density [6,7]. Here we explore for the first time the prospects for its detection.

For concreteness, we consider the simplest UED model, with one extra dimension of size $R \sim \text{TeV}^{-1}$ compactified on an S^1/Z_2 orbifold. At the lowest order, the KK masses are simply the momenta along the extra dimension and are quantized in units of $1/R$. The degeneracy at each KK level is lifted by radiative corrections and boundary terms [4]. The boundaries also break momentum conservation in the extra dimension down to a Z_2 parity, under which KK modes with odd KK number are charged. This KK-parity corresponds to the symmetry of reflection about the midpoint in the extra dimension; it is anomaly free and not violated by quantum gravity effects. KK-parity conservation implies that the lightest KK particle is stable. KK partners of electroweak gauge bosons and neutrinos are then all possible dark matter candidates. We consider B^1 , the first KK mode of the hypercharge gauge boson, which at one loop is naturally the lightest KK mass eigenstate in minimal models [4,5].

In this UED scenario, constraints from precision data require only $1/R \geq 300$ GeV [2]. Collider searches are also quite challenging: the Tevatron Run II may probe slightly beyond this bound and the LHC may reach $1/R \sim 1.5$ TeV [5]. Dark matter searches provide another possibility for probing these models and differentiating them from other new physics.

For a given KK spectrum, the B^1 thermal relic density may be accurately determined [6]. B^1 s annihilate effectively through s -wave processes, unlike neutralinos, and so the desired thermal relic density is obtained for higher masses than typical for neutralinos. If B^1 s are the only KK modes with significant abundance at the freezeout temperature, the desired relic density is found for $m_{B^1} \approx 1$ TeV. However, many other KK states may be closely degenerate with B^1 , and their presence at freezeout will modify this conclusion. KK quarks and gluons annihilate with much larger cross sections through strong interactions, and so increase the predicted m_{B^1} . On the other hand, degenerate KK leptons lower the average annihilation cross section and require lower m_{B^1} . In addition to

the cosmological assumptions present in all relic density calculations, the B^1 relic density is therefore rather model-dependent, with the optimal m_{B^1} ranging from several hundred GeV to a few TeV, depending sensitively on the KK spectrum. Here we study the prospects for detection in a model-independent way by considering m_{B^1} as a free parameter in the appropriate range.

We first consider the direct detection of B^1 dark matter. Dark matter particles are currently nonrelativistic, with velocity $v \sim 10^{-3}$. For weak-scale dark matter, the recoil energy from scattering off nuclei is ~ 0.1 MeV, and far less for scattering off electrons. We therefore consider elastic scattering off nucleons and nuclei.

At the quark level, B^1 scattering takes place through KK quarks, with amplitude $\mathcal{M}_{q_i}^{q_1} = \mathcal{M}_{q_L}^{q_1} + \mathcal{M}_{q_R}^{q_1}$, where

$$\mathcal{M}_{q_i}^{q_1} = -i \frac{e^2}{\cos^2 \theta_W} Y_{q_i}^2 \varepsilon_\mu^*(p_3) \varepsilon_\nu(p_1) \times \bar{u}(p_4) \left[\frac{\gamma^\mu k_1 \gamma^\nu}{k_1^2 - m_{q_i}^2} + \frac{\gamma^\nu k_2 \gamma^\mu}{k_2^2 - m_{q_i}^2} \right] P_i u(p_2), \quad (1)$$

$Y = Q - I$ is hypercharge, $k_1 = p_1 + p_2$, and $k_2 = p_2 - p_3$; and through Higgs exchange, with amplitude

$$\mathcal{M}_q^h = i \frac{e^2}{2 \cos^2 \theta_W} \frac{m_f}{k_3^2 - m_h^2} \varepsilon_\mu^*(p_3) \varepsilon^\mu(p_1) \bar{u}(p_4) u(p_2), \quad (2)$$

where $k_3 = p_1 - p_3$. In the extreme nonrelativistic limit, $p_1 = p_3 = (m_{B^1}, \mathbf{0})$, and expanding to linear order in $p_2 = (E_q, \mathbf{p}_q)$, these amplitudes then reduce to

$$\mathcal{M}_q^{q_1} \approx \alpha_q \varepsilon_\mu^*(p_3) \varepsilon_\nu(p_1) \varepsilon^{0\mu\nu\rho} \xi_4^\dagger \frac{\sigma_\rho}{2} \xi_2 - i \beta_q \varepsilon_\mu^*(p_3) \varepsilon^\mu(p_1) \xi_4^\dagger \xi_2, \quad (3)$$

$$\mathcal{M}_q^h \approx -i \gamma_q \varepsilon_\mu^*(p_3) \varepsilon^\mu(p_1) \xi_4^\dagger \xi_2, \quad (4)$$

where ξ_4 and ξ_2 are two-component spinors, and

$$\alpha_q = \frac{2e^2}{\cos^2 \theta_W} \left[\frac{Y_{q_L}^2 m_{B^1}}{m_{q_L}^2 - m_{B^1}^2} + (L \rightarrow R) \right], \quad (5)$$

$$\beta_q = E_q \frac{e^2}{\cos^2 \theta_W} \left[Y_{q_L}^2 \frac{m_{B^1}^2 + m_{q_L}^2}{(m_{q_L}^2 - m_{B^1}^2)^2} + (L \rightarrow R) \right], \quad (6)$$

$$\gamma_q = m_q \frac{e^2}{2 \cos^2 \theta_W m_h^2}. \quad (7)$$

The interactions divide into spin-dependent and spin-independent parts [8]. Higgs exchange contributes to scalar couplings, while q^1 exchange contributes to both. Note that the two contributions to scalar interactions interfere constructively; barring extremely heavy KK masses, there is an inescapable lower bound on both spin-dependent and scalar cross sections.

The spin-dependent coupling is $\alpha_q \mathbf{S}_{B^1} \cdot \mathbf{S}_q$, where \mathbf{S}_{B^1} and \mathbf{S}_q are spin operators. We must evaluate this matrix element between nucleon or nucleus bound states. By the

Wigner-Eckart theorem, we may replace \mathbf{S}_q by $\lambda_q \mathbf{J}_N$, where \mathbf{J}_N is the nucleon or nuclear spin operator. The constant of proportionality is

$$\lambda_q = \Delta_q^p \langle S_p \rangle / J_N + \Delta_q^n \langle S_n \rangle / J_N. \quad (8)$$

$\Delta_q^{p,n}$ is given by $\langle p, n | \mathbf{S}_q^\mu | p, n \rangle \equiv \Delta_q^{p,n} \mathbf{S}_{p,n}^\mu$ and is the fraction of the nucleon spin carried by quark q . A recent analysis finds $\Delta_u^p = \Delta_d^n = 0.78 \pm 0.02$, $\Delta_u^n = \Delta_d^p = -0.48 \pm 0.02$, and $\Delta_s^p = \Delta_s^n = -0.15 \pm 0.02$ [9]. $\langle S_{p,n} \rangle / J_N \equiv \langle N | S_{p,n} | N \rangle / J_N$ is the fraction of the total nuclear spin J_N that is carried by the spin of protons or neutrons. For scattering off protons and neutrons, λ_q reduces to Δ_q^p and Δ_q^n , respectively.

The spin-dependent cross section is $m_N^2 / [4\pi(m_{B^1} + m_N)^2] |\langle \mathcal{M} \rangle|^2$, where $\mathcal{M} = \sum_q \mathcal{M}_q$ and $\langle \rangle$ denotes an average over initial polarizations and sum over final polarizations. Using $\langle (\mathbf{S}_{B^1} \cdot \mathbf{J}_N)^2 \rangle = \frac{2}{3} J_N (J_N + 1)$, we find

$$\sigma_{\text{spin}} = \frac{1}{6\pi} \frac{m_N^2}{(m_{B^1} + m_N)^2} J_N (J_N + 1) \left[\sum_{u,d,s} \alpha_q \lambda_q \right]^2, \quad (9)$$

where α_q and λ_q are given in Eqs. (5) and (8).

The spin-independent cross section is

$$\sigma_{\text{scalar}} = \frac{m_N^2}{4\pi (m_{B^1} + m_N)^2} [Z f_p + (A - Z) f_n]^2, \quad (10)$$

where Z and A are nuclear charge and atomic number,

$$f_p = \sum_{u,d,s} (\beta_q + \gamma_q) \langle p | \bar{q} q | p \rangle = \sum_{u,d,s} \frac{\beta_q + \gamma_q}{m_q} m_p f_{T_q}^p, \quad (11)$$

and similarly for f_n . We take $f_{T_u}^p = 0.020 \pm 0.004$, $f_{T_d}^p = 0.026 \pm 0.005$, $f_{T_u}^n = 0.014 \pm 0.003$, $f_{T_d}^n = 0.036 \pm 0.008$, and $f_{T_s}^{p,n} = 0.118 \pm 0.062$ [10]. E_q of Eq. (6) is the energy of a bound quark and is rather ill defined. In evaluating Eq. (11), we conservatively replace E_q by the current mass m_q . We also neglect couplings to gluons mediated by heavy quark loops; a detailed loop-level analysis along the lines of Refs. [11,12] for neutralinos is in progress [13]. Given the constructive interference noted above, these contributions can only increase the cross section.

We present both spin-independent and spin-dependent cross sections in Fig. 1. We assume that all first level KK quarks are degenerate with mass m_{q^1} . Proton cross sections are given; neutron cross sections are similar for spin-dependent interactions and almost identical for scalar cross sections. The cross sections are large for low m_{B^1} . They are also strikingly enhanced by r^{-2} for small $r \equiv (m_{q^1} - m_{B^1}) / m_{B^1}$ when scattering takes place near an s -channel pole. Such degeneracy is unmotivated in general, but is natural for UED models, where all KK particles are highly degenerate at tree level.

Projected sensitivities of near future experiments are also shown in Fig. 1. For scattering off individual nucleons, scalar cross sections are suppressed relative to

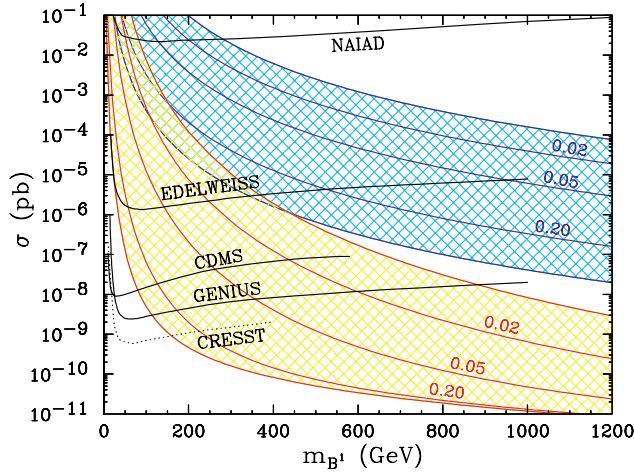


FIG. 1 (color online). Predicted spin-dependent proton cross sections (dark-shaded, blue), along with the projected sensitivity of a 100 kg NAIAD array [14]; and predicted spin-independent proton cross sections (light-shaded, red), along with the current EDELWEISS sensitivity [15], and projected sensitivities of CDMS [16], GENIUS [17], and CRESST [18]. (The CRESST projection is long-term and conditional upon increased exposure and improved background rejection.) The predictions are for $m_h = 120$ GeV and $0.01 \leq r = (m_{q^1} - m_{B^1})/m_{B^1} \leq 0.5$, with contours for specific intermediate r labeled.

spin-dependent ones by $\sim m_p/m_{B^1}$. However, this effect is compensated in large nuclei where spin-independent rates are enhanced by $\sim A^2$. In the case of bosonic KK dark matter, the latter effect dominates, and the spin-independent experiments have the best prospects for detection, with sensitivity to m_{B^1} far above current limits.

Dark matter may also be detected when it annihilates in the galactic halo, leading to positron excesses in space-based and balloon experiments. The positron flux is [19]

$$\frac{d\Phi_{e^+}}{d\Omega dE} = \frac{\rho^2}{m_{B^1}^2} \sum_i \langle \sigma_i v \rangle B_{e^+}^i \int dE_0 f_i(E_0) G(E_0, E), \quad (12)$$

where ρ is the local dark matter mass density, the sum is over all annihilation channels i , and $B_{e^+}^i$ is the e^+ branching fraction in channel i . The initial positron energy distribution is given by $f(E_0)$, and the Green function $G(E_0, E)$ propagates positrons in the galaxy.

Several channels contribute to the positron flux. Here we focus on the narrow peak of primary positrons from direct $B^1 B^1 \rightarrow e^+ e^-$ annihilation. (Annihilation to muons, taus, and heavy quarks also yield positrons through cascade decays, but with relatively soft and smeared spectra.) In this case, the source is monoenergetic, and Eq. (12) simplifies to

$$\frac{d\Phi_{e^+}}{d\Omega dE} = 2.7 \times 10^{-8} \text{ cm}^{-2} \text{ s}^{-1} \text{ sr}^{-1} \text{ GeV}^{-1} \frac{\langle \sigma_{ee} v \rangle}{\text{pb}} \times \left[\frac{\rho}{0.3 \text{ GeV/cm}^3} \right]^2 \left[\frac{1 \text{ TeV}}{m_{B^1}} \right]^2 g\left(1, \frac{E}{m_{B^1}}\right), \quad (13)$$

where the annihilation cross section is

$$\langle \sigma_{ee} v \rangle = \frac{e^4}{9\pi \cos^4 \theta_W} \left[\frac{Y_{e_L}^4}{m_{B^1}^2 + m_{e_L}^2} + (L \rightarrow R) \right], \quad (14)$$

and the reduced Green function g is as in Ref. [20].

Positron spectra and an estimated background (model C from Ref. [19]) are given in Fig. 2. The sharp peak at $E_{e^+} = m_{B^1}$ is spectacular—while propagation broadens the spectrum, the monoenergetic source remains evident. This feature is extremely valuable, as the background, although resulting from many sources, should be smooth. Maximal E_{e^+} also enhances detectability since the background drops rapidly with energy. Both of these virtues are absent for neutralinos, where Majoraneness implies helicity-suppressed annihilation amplitudes, and positrons are produced only in cascades, leading to soft, smooth spectra [21]. A peak in the e^+ spectrum will not only be a smoking gun for B^1 dark matter, it will also exclude neutralinos as the source.

Of the many positron experiments, the most promising is AMS [22], the antimatter detector to be placed on the International Space Station. AMS will distinguish positrons from electrons even at 1 TeV energies [23]. With aperture $6500 \text{ cm}^2 \text{ sr}$ and a runtime of 3 yr, AMS will detect ~ 1000 positrons with energy above 500 GeV, and may detect a positron peak from B^1 dark matter.

Photons from dark matter annihilation in the center of the galaxy also provide an indirect signal. The line signal from $B^1 B^1 \rightarrow \gamma\gamma$ is loop suppressed, and so we consider continuum photon signals. The integrated photon flux above some photon energy threshold E_{th} is [20]

$$\Phi_\gamma(E_{\text{th}}) = 5.6 \times 10^{-12} \text{ cm}^{-2} \text{ s}^{-1} \bar{J}(\Delta\Omega) \Delta\Omega \times \left[\frac{1 \text{ TeV}}{m_{B^1}} \right]^2 \sum_q \frac{\langle \sigma_{qq} v \rangle}{\text{pb}} \int_{E_{\text{th}}}^{m_{B^1}} dE \frac{dN_\gamma^q}{dE}, \quad (15)$$

where the sum is over all quark pair annihilation channels

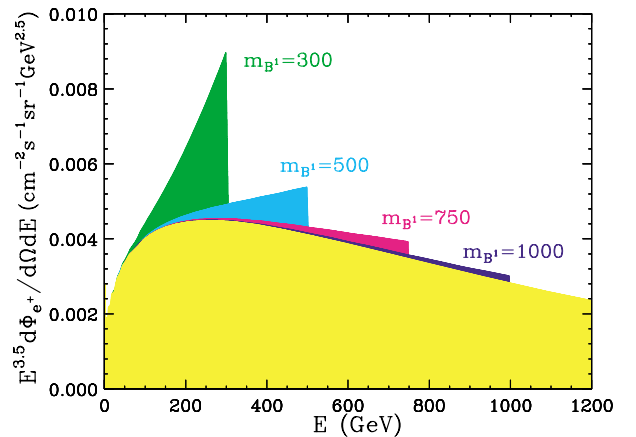


FIG. 2 (color online). Predicted positron signals above background (light shaded area, yellow) as a function of positron energy for $m_{B^1} = m_{e_L^1} = m_{e_R^1} = 300, 500, 750,$ and 1000 GeV.

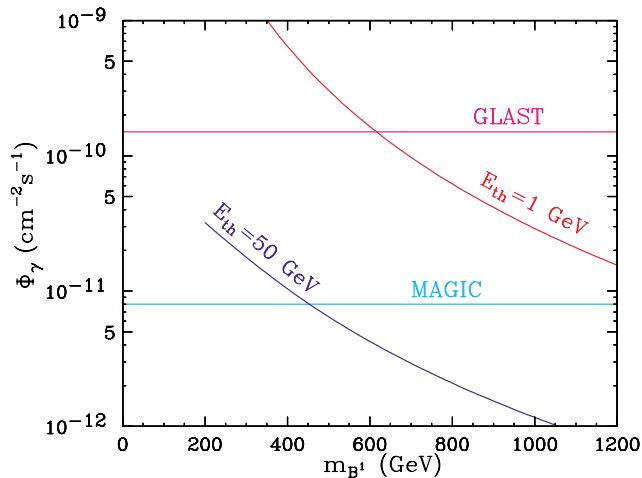


FIG. 3 (color online). Integrated photon flux as a function of m_{B^1} for energy thresholds of 1 and 50 GeV. Projected sensitivities for GLAST and MAGIC are also shown.

[with cross sections similar to Eq. (14)], and dN_γ^q/dE is the differential gamma ray multiplicity for channel qq . The hardest spectra result from fragmentation of light quarks [24], and so the lack of chirality suppression again gives a relative enhancement over neutralinos. $\Delta\Omega$ is the solid angle of the field of view of a given telescope, and \bar{J} is a measure of the cuspsiness of the galactic halo density profile. There is a great deal of uncertainty in \bar{J} , with possible values in the range 3 to 10^5 . We choose $\Delta\Omega = 10^{-3}$ and a moderate value of $\bar{J} = 500$.

Integrated photon fluxes are given in Fig. 3 for two representative E_{th} : 1 GeV, accessible to space-based detectors, and 50 GeV, characteristic of ground-based telescopes. Estimated sensitivities for two of the more promising experiments, GLAST [25] and MAGIC [26], are also shown. We find that photon excesses are detectable for $m_{B^1} \lesssim 600$ GeV. Note that these signals may be greatly enhanced for clumpy halos with large \bar{J} .

Finally, high-energy neutrinos from annihilating dark matter trapped in the core of the Sun or the Earth, can be detected through their charged-current conversion to muons. Unlike the case in supersymmetry, B^1 s can annihilate directly to neutrinos, with branching ratio $\approx 1.2\%$. Secondary neutrinos may also result from final states with heavy quarks, charged leptons, or Higgs bosons. Considering primary neutrinos and those from tau decays from the Sun (which is typically full, with capture and annihilation in equilibrium), we find that, for $r = 0.5$ (0.02), next generation neutrino telescopes such as AMANDA, NESTOR, and ANTARES will probe m_{B^1} up to 200 GeV (600 GeV) and IceCube will be sensitive to $m_{B^1} = 400$ GeV (1400 GeV) [13].

In conclusion, we find excellent prospects for KK dark matter detection. The elastic scattering cross sections are enhanced near s -channel KK resonances, providing good chances for *direct* detection. In addition, *indirect* detec-

tion is typically much more promising than in supersymmetry for three reasons. First, there is no helicity suppression for the annihilation of bosonic KK dark matter into fermion pairs. Second, the preferred B^1 mass range is higher than in supersymmetry, leading to harder positron, photon, and neutrino spectra, with better signal-to-background ratio. And third, B^1 annihilation produces primary positrons and neutrinos with distinctive energy spectrum shapes, again facilitating observation above background. Kaluza-Klein gauge bosons therefore provide a promising and qualitatively new possibility for dark matter and dark matter searches.

- [1] T. Kaluza, Sitzungsber. Preuss. Akad. Wiss. Berl. Math. Phys. **K1**, 966 (1921); O. Klein, Z. Phys. **37**, 895 (1926) [Surv. High-Energy Phys. **5**, 241 (1986)].
- [2] T. Appelquist, H.-C. Cheng, and B. A. Dobrescu, Phys. Rev. D **64**, 035002 (2001).
- [3] K. R. Dienes, E. Dudas, and T. Gherghetta, Nucl. Phys. **B537**, 47 (1999).
- [4] H.-C. Cheng, K. T. Matchev, and M. Schmaltz, Phys. Rev. D **66**, 036005 (2002).
- [5] H.-C. Cheng, K. T. Matchev, and M. Schmaltz, hep-ph/0205314.
- [6] G. Servant and T. M. Tait, hep-ph/0206071.
- [7] See also E. W. Kolb and R. Slansky, Phys. Lett. B **135**, 378 (1984); J. Saito, Prog. Theor. Phys. **77**, 322 (1987).
- [8] M. W. Goodman and E. Witten, Phys. Rev. D **31**, 3059 (1985).
- [9] G. K. Mallot, Int. J. Mod. Phys. A **15S1**, 521 (2000).
- [10] J. R. Ellis, A. Ferstl, and K. A. Olive, Phys. Lett. B **481**, 304 (2000).
- [11] M. Drees and M. Nojiri, Phys. Rev. D **48**, 3483 (1993).
- [12] M. Drees and M. M. Nojiri, Phys. Rev. D **47**, 376 (1993).
- [13] H.-C. Cheng, J. L. Feng, and K. T. Matchev (to be published).
- [14] N. J. Spooner *et al.*, Phys. Lett. B **473**, 330 (2000).
- [15] A. Benoit *et al.*, astro-ph/0206271.
- [16] R. W. Schnee *et al.*, Phys. Rep. **307**, 283 (1998).
- [17] H. V. Klapdor-Kleingrothaus, hep-ph/0104028.
- [18] CRESST-Collaboration, M. Bravin *et al.*, Astropart. Phys. **12**, 107 (1999).
- [19] I. V. Moskalenko and A. W. Strong, Phys. Rev. D **60**, 063003 (1999).
- [20] J. L. Feng, K. T. Matchev, and F. Wilczek, Phys. Rev. D **63**, 045024 (2001).
- [21] J. R. Ellis *et al.*, Eur. Phys. J. C **24**, 311 (2002).
- [22] AMS Collaboration, A. Barrau *et al.*, astro-ph/0103493.
- [23] H. Hofer and M. Pohl, Nucl. Instrum. Methods Phys. Res., Sect. A **416**, 59 (1998).
- [24] L. Bergstrom, P. Ullio, and J. H. Buckley, Astropart. Phys. **9**, 137 (1998).
- [25] H. F. Sadrozinski, Nucl. Instrum. Methods Phys. Res., Sect. A **466**, 292 (2001).
- [26] MAGIC Collaboration, M. Martinez *et al.*, in *Proceedings of ICRC99, Utah, 1999* (OG.4.3.08).